Available online at www.sciencedirect.com

ScienceDirect

journal homepage: www.elsevier.com/locate/jasi

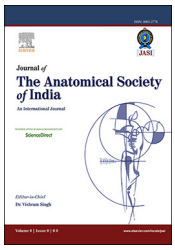

Original Article

Age-related changes in the ductular system and stellate cells of human pancreas

Shubhi Saini [a], *Tony George Jacob* [b], *D.N. Bhardwaj* [c], *Tara Sankar Roy* [d,*]

[a] Ph.D. Student, Department of Anatomy, All India Institute of Medical Sciences, Ansari Nagar, New Delhi, India
[b] Assistant Professor, Department of Anatomy, All India Institute of Medical Sciences, Ansari Nagar, New Delhi, India
[c] Professor, Department of Forensic Medicine, All India Institute of Medical Sciences, Ansari Nagar, New Delhi, India
[d] Professor, Department of Anatomy, All India Institute of Medical Sciences, Ansari Nagar, New Delhi, India

ARTICLE INFO

Article history:
Received 15 September 2015
Accepted 26 October 2015

Keywords:
Pancreatic ducts
Aging
Fibrosis
Immunohistochemistry
Chronic pancreatitis

ABSTRACT

Introduction: Age associated progressive fibrosis may be a major causative factor that leads to pathogenesis of many diseases. Activated pancreatic stellate cells (α-SMA positive) play a major role in fibrogenesis that affects the cytoarchitecture and functioning of pancreas. This study dealt with age-related fibrotic changes in the ductular system of the tail and body of pancreas and the morphology of pancreatic stellate cells.

Methods: Pancreata ($n = 36$) from cadavers aged 30–80 years were obtained after due clearances and processed for Masson's trichome staining. Fibrosis was quantified using Adobe Photoshop (CS2) and Image-J software. Hierarchical cluster analysis was done on the luminal area and total ductal area that were measured by the nucleator probe of StereoInvestigator software (MBF, Vermont, USA). Pancreatic stellate cells (α-SMA positive cells) were identified by immunohistochemistry and quantified stereologically around periacinar, periductular, perivascular, and peri-Islet areas.

Results: An increased fibrosis was noted in body and tail regions of the pancreas with increasing age. Three duct populations were identified in clustering. Their area and corresponding lumen showed a significant increase with progressive decades ($p < 0.001$). α-SMA positive cells increased significantly from 4th to 7th decades ($p = 0.002$, 0.004 and 0.002, respectively).

Discussion: Pancreatic stellate cells may be important contributors to increased fibrosis in pancreas. The classification of pancreatic ducts into three clusters may serve to be a useful tool.

1. Introduction

Progressive fibrosis is a characteristic of aging in organs such as liver, kidney,[1] lung,[2] and pancreas.[3] Fibrosis is the excessive accumulation of extracellular matrix (ECM) proteins as a result of imbalance between the deposition and degradation of ECM.[4] The accumulating ECM affects tissue function that leads to the progression of fibrosis, often as a vicious cycle.

In the pancreas, fibrosis may contribute to the initiation of disease by deposition of ECM, production of cytokines, and

* *Corresponding author.*
E-mail addresses: tsroyaiims@gmail.com, tsroy@aiims.ac.in (T.S. Roy).
http://dx.doi.org/10.1016/j.jasi.2015.10.011

restriction of blood flow. These changes destroy the tissue structure and cause degeneration of the gland,[5] which affects the functioning of its exocrine and endocrine components.[6] Fibrosis is also an important component of chronic pancreatitis,[23] pancreatic cancer[5] and type 2 Diabetes Mellitus.[7] Many workers have observed progressive fibrosis occurring in the pancreas with age.[8,9,26] In addition, some researchers have found pancreatographic changes in the ductal system of the pancreas.[22,25] In the European population, fibrotic changes start at a relatively late age around 60 years[12] than what is seen in Indian people.[10] The quantitative study of[11] using colorimetric method found a significant correlation between collagen and degree of fibrosis in pancreas. The presence of myofibroblast-like cells, in association with the fibrotic foci, indicates an ongoing fibrogenic process.[12] It has been reported that these myofibroblast-like cells called pancreatic stellate cells (PSC) play a major role in pancreatic fibrogenesis.[4]

The similarities of PSCs with hepatic stellate cells and their association with fibrotic areas suggest that PSCs participate in the development of pancreatic fibrosis.[13] Activated PSCs are found in areas of extensive necrosis and inflammation that are associated with cytokines, growth factors, and reactive oxygen species.[14] Animal models of experimental pancreatitis[15,16] indicate that parenchymal necrosis, and inflammation takes place before the activation of PSCs. These activated PSCs proliferate, migrate, and deposit ECM proteins.[5] It would be interesting to determine, whether the increasing fibrosis observed in the aging pancreas has a similar pathogenesis as in other diseases causing fibrosis of the pancreatic tissue. One of the methods of assessment of the extent of fibrosis in the tissues is by specifically staining for fibrous tissue in histological sections. A simple histological staining technique such as Masson's Trichrome can differentiate the fibrous component in the tissues. Further, immunohistochemistry for the identification of activated stellate cells that express α-smooth muscle actin (α-SMA), glial fibril associated protein (GFAP), etc.,[14] would determine, if these cells are located at the sites of fibrosis.[17]

To the best of our knowledge, there are no studies from India that have recorded age-related fibrotic changes in the human pancreas. The results could provide useful insights upon the progression of various diseases that seem to appear as a part of the aging process, particularly type 2 Diabetes Mellitus.

In the present study, we have determined the relationship between age, fibrosis, and alterations in the morphology of the various components of the pancreas. We have also morphometrically classified the pancreatic ducts into three clusters according to their luminal and ductal areas. We also attempted to determine a fibrogenic mechanism by quantifying PSC around periacinar, periductular, periacinar and periislar areas.

2. Materials and methods

Thirty-six adult human pancreata were collected from the mortuary at the Department of Forensic Medicine, All India Institute of Medical Science, New Delhi (AIIMS), in accordance with the protocol approved by the Institutional Human Ethics Committee. The pancreatic tissue samples from age group of 30–80 were taken and divided into four groups (4th, 5th, 6th, and 7th decades). Samples of known alcoholic, chronic smoker, pancreatic, metabolic, and hepatobiliary disease, traumatic injury and unclaimed bodies were excluded. The body and tail parts of the pancreas were excised from the cadavers, washed with normal saline and fixed in 4% buffered paraformaldehyde (pH 7.4) at 4 °C. After initial fixation, the body and tail of the pancreas were sectioned in the sagittal plane. One of the numerous parasagittal sections was randomly selected and further sectioned in the coronal plane into three equidistant segments. These segments were further divided into equal portions depending on the original length of the segments (Supplementary Fig. 1). These blocks were processed for paraffin embedding. Thereafter, 5 μm sections of these tissue blocks were cut on a rotary microtome and stained with Masson's trichrome.

Supplementary Fig. 1 related to this article can be found, in the online version, at doi:10.1016/j.jasi.2015.10.011.

2.1. *Microscopy and Image analysis for quantification of fibrosis.*

Masson's trichrome stained slides were viewed under, 10× and 40× objectives of a BX61 Olympus microscope for qualitative and semi-quantitative assessment of fibrosis. From each slide, 6–8 high power fields were systematically and randomly selected and images were clicked with a CX9000 digital camera attached to the microscope. The digital images were processed using the Adobe Photoshop software (v7) with the purpose of mapping the fibrotic areas by selecting the pseudocolor of the fibrotic areas, stained green (collagen) with Masson's trichrome, with a color-picker tool (Supplementary Fig. 2). This picked up all the areas in a similar shade of green, wherein the selectivity of the color was kept at 80% accuracy in order to pick up all areas of fibrosis and the variability that arises from performing the staining in different batches. The color of the fibrotic areas was made more distinct by adjusting the fuzziness. Each image was then imported to Image J Basics software, version 1.38 (http://rsb.info.nih.gov/ij/). The image was then converted to gray scale, which converts the image to 256 (8 bit) shades of gray. Thresholding of the image was done by converting to binary image (black/white) by defining gray scale cut off point. In this scale 0 (zero) is pure black and 255 is pure white. Gray scale values below the cut off become black and those above become white. By this procedure all the fibrotic areas in the field appeared black (Supplementary Fig. 2c). These black areas were the stained areas of fibrosis and were measured in this program. The percentage of fibrotic areas in each field was computed as follows:

$$\text{Percentage of fibrotic area} = \text{Total Fibrotic area(Black)}/\text{Total Image area(White)} \times 100.$$

Supplementary Fig. 2 related to this article can be found, in the online version, at doi:10.1016/j.jasi.2015.10.011.

2.2. Computing the fibrotic area around the duct

In order to estimate the fibrotic area around ducts in the pancreas, we used the nucleator probe of the StereoInvestigator software (Micro Bright Field, VA, USA). Briefly, 6–8 random fields were selected, and the cross-sectional areas of duct and lumen were measured using the nucleator probe. A marker was selected and on clicking with a mouse, in the duct, four rays emerged. The limits of the lumen of the duct, its wall and the extent of fibrous tissue were marked on the rays (Supplementary Fig. 3). The regions measured were: (a) Duct area (lumen + epithelium of the duct and the fibrous tissue around the duct) (b) only lumen, (c) Wall of the duct [Duct area (a) − lumen area (b)].

Supplementary Fig. 3 related to this article can be found, in the online version, at doi:10.1016/j.jasi.2015.10.011.

2.3. Immunohistochemistry

Paraffin sections of the pancreas were deparaffanized, rehydrated, and washed in phosphate buffered saline containing 0.5% Tween20 (washing buffer). Antigen was retrieved by boiling the sections for 10 min in citrate buffer (pH 8), endogenous peroxidase activity was blocked by incubation with 3% H_2O_2. After washing, sections were incubated in 1.5% normal horse serum (host species of secondary antibody + 1% bovine serum albumin) for 60 min. Sections were then incubated with primary antibody (anti-α-smooth muscle actin, dilution 1:200; mouse monoclonal, Abcam-ab54723) antibody for 60 min at room temperature, washed and then were incubated for 30 min at room temperature with biotinylated secondary antibody followed by HRP-conjugated ABC reagent for 30 min. Thereafter, a solution of diaminobenzidine (DAB) and H_2O_2 was added to reveal the sites of binding of the primary antibody by a brown color. The sections were counterstained, dehydrated, and mounted. The sections were nalyzed using the StereoInvestigator software. Initially, the area of the pancreatic and islar tissue were identified under the microscope and separately marked out under low magnification. The area of these tissues were estimated by the Cavalieri probe in the software. Thereafter, the α-SMA positive cells were counted using different markers for brown stained cells identified in the perivascular, periductular and peri-islar regions of the pancreas. Their numerical density of perivascular and periductular α-SMA positive cells was calculated by dividing the total number of cells counted in 6–8 different high power fields by the area of the pancreatic tissue; whereas the numerical density of peri-islar α-SMA positive cells was calculated by dividing the total number of these cells by the area of the islets of Langerhans.

2.4. Statistical analysis

Data were represented as mean (standard error). Parametric data of different groups were compared to each other using One-way Analysis of Variance (ANOVA) and post hoc analysis was made by Tukey's test. For non-parametric data, the various groups were compared to each other using Kruskal–Wallis test and inter group analysis was made by Mann–Whitney *U*-test. Significance was set at an overall *p*-value less than 0.05.

Hierarchical cluster analysis was performed on the two diameters of the duct-internal lumen and external (epithelium up to the limit of fibrous tissue). This was done to identify different populations of the duct and whether the extent of fibrosis was different in the varied populations of the ducts in the different age groups.

The analysis was performed using SPSS (version 15, Chicago, Ilinois, USA).

3. Results

The pancreas grossly appeared to be fleshy and lobulated with a thickened connective tissue capsule in the aged population (6th and 7th decades). No other macroscopic changes were visible. Microscopically, the pancreatic acinar cells did not show any remarkable changes across the ages. Histological changes such as periductular fibrosis, acinar atrophy, fatty infiltration, and ductal ectasias and papillary hyperplasia were seen to increase with age. Fibrous tissue was found around the ducts, vessels, acini and in the islets of Langerhans and increased remarkably with increasing age that was observed as bluish green stained tissue as seen in Masson's trichome stained sections (Fig. 1).

3.1. Quantification of fibrosis

Quantification was done and it was found that there was no significant difference in fibrosis between the various parts of the pancreas that we had studied, namely the anterior, central, and posterior parts of the body, and the tail ($p > 0.05$) (Fig. 2, Table 1).

Overall, pancreata of the 7th decade showed higher fibrosis in all parts of the pancreas studied, when compared to the other age groups Fig. 1(d).

3.2. Fibrosis around the ducts

The wall of the duct includes the epithelial lining along with the fibrous tissue around the duct. An increase in fibrosis was noted in the walls of ducts from 4th to 7th decade (Fig. 3, Table 2). The fibrosis was significantly higher in the 5th decade in comparison to 4th decade ($p < 0.01$). The increase in the periductular fibrosis in the 6th decade was not significantly more than that of the 5th decade ($p > 0.05$). However, there was a significant increase in the fibrosis observed in pancreata of the 7th decade ($p < 0.01$) (Fig. 3).

The area of the lumen of the duct also increased significantly with increasing age ($p < 0.01$). A marked increase of the lumen of the duct was noticed during 7th decade with respect to 4th and 5th decades ($p < 0.01$) (Table 2).

3.3. Classification of the ducts by hierarchical cluster analysis

The scatter plot identified three populations of ducts, which were color coded (Fig. 4). Area of three duct populations and their corresponding lumen were shown to be significantly

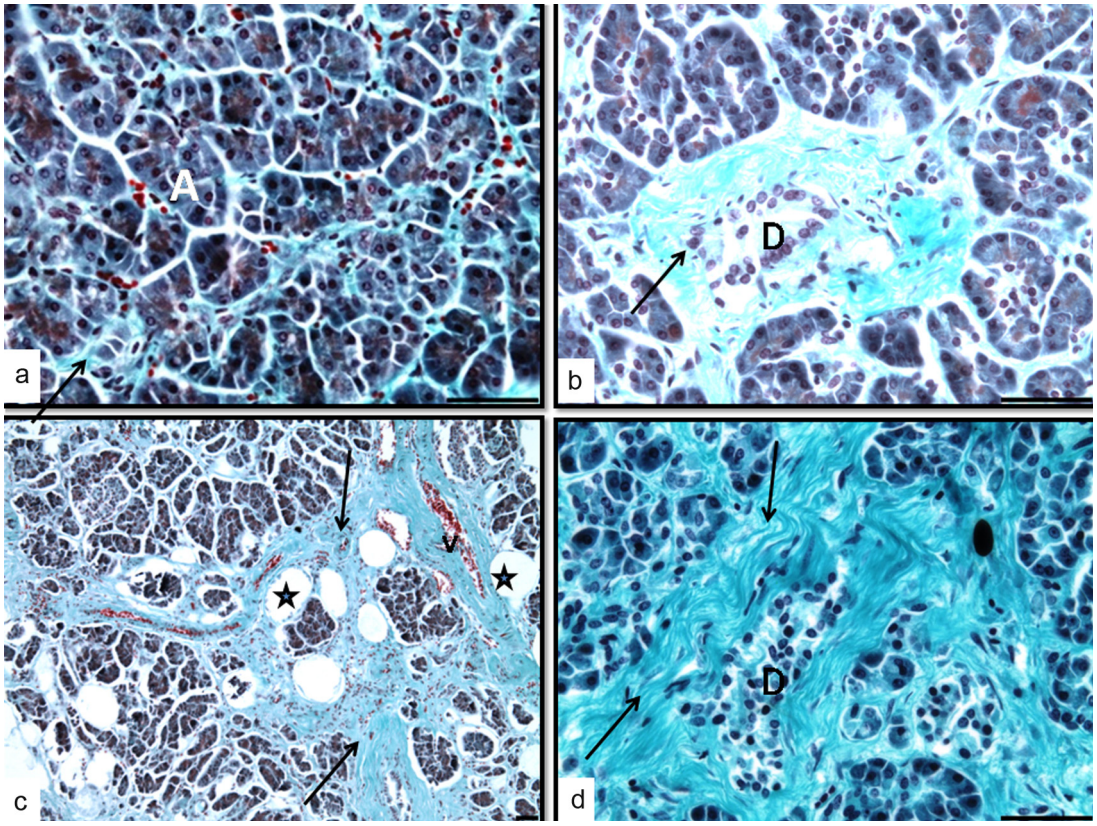

Fig. 1 – Photomicrograph of sections of pancreas stained by Masson's Trichome method showing pancreatic acini (A), duct (D) and connective around acini and ducts (green, arrow) in (a) 36 years, (b) 45 years, (c) 52 years, and (d) 61 years. Scale bar: (a) and (b) 20 μm, (c) 50 μm, and (d) 20 μm.

increased with increasing age (Table 2) ($p < 0.001$ for duct wall area and $p < 0.001$ for lumen area, respectively) (by Tukey's inter-group comparison).

3.4. *Quantitative assessment of the positive α-SMA cells*

A number of α-SMA positive cells in the periacinar, periductular, perivascular and in the islets in the various decades have been compiled in Table 3 and shown in Fig. 5. It reveals that the periacinar α-SMA cells exhibit a significant increase in number from 4th to 7th decade ($p = 0.002$). The distribution of α-SMA positive cells in the perivascular ($p = 0.002$) and periductular ($p = 0.004$) also increased significantly from the 4th to 7th decade. Their population in the peri-islar area also showed significant increase with age ($p = 0.012$).

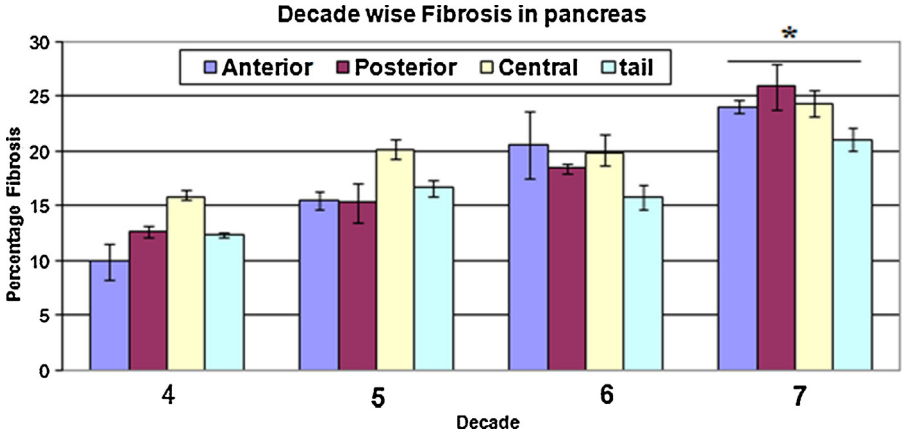

Fig. 2 – Graphical representation of fibrosis in different regions of pancreas. The fibrosis in the different regions of the pancreas was significantly more (*) in the 7th decade when compared to the other decades. (anterior: $p = 0.01$; central: $p = 0.012$; posterior: $p = 0.008$; and tail: $p = 0.005$).

Table 1 – Mean percentage of fibrotic areas in different regions of the pancreas at different ages.

Decade	Region			
	Anterior (%)[a]	Posterior (%)[a]	Central (%)[a]	Tail (%)[a]
Fourth	9.96 (1.70)	12.67 (0.50)	15.82 (0.77)	12.41 (0.21)
Fifth	15.55 (0.75)	15.31 (1.8)	20.19 (0.95)	16.70 (0.76)
Sixth	20.62 (3.02)	18.52 (0.45)	19.89 (1.75)	15.84 (1.15)
Seventh	24.10 (0.60)*	25.92 (2.10)*	24.33 (1.32)*	21.10 (1.06)*
Total	17.21 (1.48)	17.76 (1.40)	19.81 (0.94)	16.27 (0.87)

* $p < 0.05$, 4th vs. 7th decades.
[a] Mean (SE).

Table 2 – Mean area of the wall of duct and its luminal area in μm^2. The hierarchical cluster analysis revealed three different populations of ducts in each decade studied.

Decade (*n*)	Duct population	Area of wall of the duct (μm^2)[a]	Area of duct lumen (μm^2)[a]
4th (51)	1	1451.29 (379.39)	601.67 (121.68)
	2	9554.50 (2120.49)	7138.4 (1348.86)
	3	16,934.73 (496.43)	13,201.25 (280.25)
5th (61)	1	2277.25 (189.01)	749.007 (116.47)
	2	12,248.5 (113.90)	6414.70 (699.96)
	3	20,389.07 (536.90)	11,533.9 (595.69)
6th (40)	1	2422.82 (229.50)	369.83 (124.77)
	2	8174.25 (617.69)	3153.82 (362.61)
	3	19,668.3 (928.29)	8931.10 (170.85)
7th (41)	1	8932.21 (1.27)	2421.46 (495.40)*
	2	39,828.9 (359.41)	15,377.37 (1699.40)*
	3	86,433.69 (2.27)	58,214.2 (7826.53)*

* $p < 0.05$ for 7th decade vs. 4th and 5th decades.
[a] Mean (SE).

4. Discussion

This study quantified the age-related changes in the distribution of pancreatic fibrosis using unbiased stereological techniques, in humans and correlated it to the occurrence of α-SMA positive PSC in different regions of the pancreatic tissue – periductular, perivascular, periacinar, and peri-islar. We believe that these cells may be important contributors to the increasing amount of fibrosis in the pancreas, and may in turn contribute to the increasing incidence of certain age-related diseases of the pancreas.[5,7] We also observed that the increasing fibrosis did not show regional differences between the body and tail of the pancreas (Table 1, Fig. 2). This morphometric study actually quantitatively proves what many radiographers and clinicians observe empirically during imaging of the pancreas that the shape and size of the ducts also markedly change with age. This study has also morphometrically classified the pancreatic ducts into three clusters according to their luminal and ductal area. This may become a tool to study pathological modifications that may affect some sub-populations of ducts more than others.[18]

In this study, we noted that the first population of ducts (in decade four, five and six as discussed in cluster analysis) constitutes mainly small ducts that showed significant progressive fibrosis. The fibrosis around the ducts (decade fifth) was doubled as compared to the 4th decade; however there was only a marginal increase in fibrosis in decade six and seven. In addition to increasing fibrosis, the luminal size also increased significantly in the 7th decade (Table 2). These observations show that there is dilation of ducts in 7th decade. Ductular ectasia, which affects interlobular and intralobular ductules, was recorded in a pancreatographic study.[10,19] Hastier et al.[24] observed that only 31.4% of elderly patients have duct diameters within defined normal limits.

The second and third population of ducts also showed significant increase in the mean ductular area along with the mean luminal area indicating an increase in the fibrosis around the duct. Schmitz-Moormann et al.[20] also noted variability in the thickness of duct wall with respect to the diameter of the ducts with aging. Therefore, our study shows that pancreatic duct fibrosis starts very early in the Indian population (4th decade) in comparison to Europeans in whom it starts usually in 6th or 7th decade.[12,25]

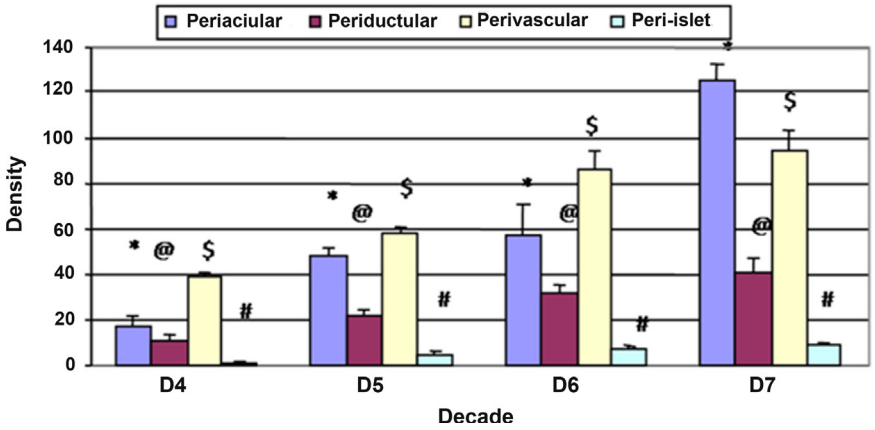

Fig. 3 – Graphical representation of density variation of positive positive α-SMA cells with age. Increase in density of α-SMA cells around the periacinar (*), periductular (@), perivascular ($) and peri-islet (#) was found to be statistically significant.

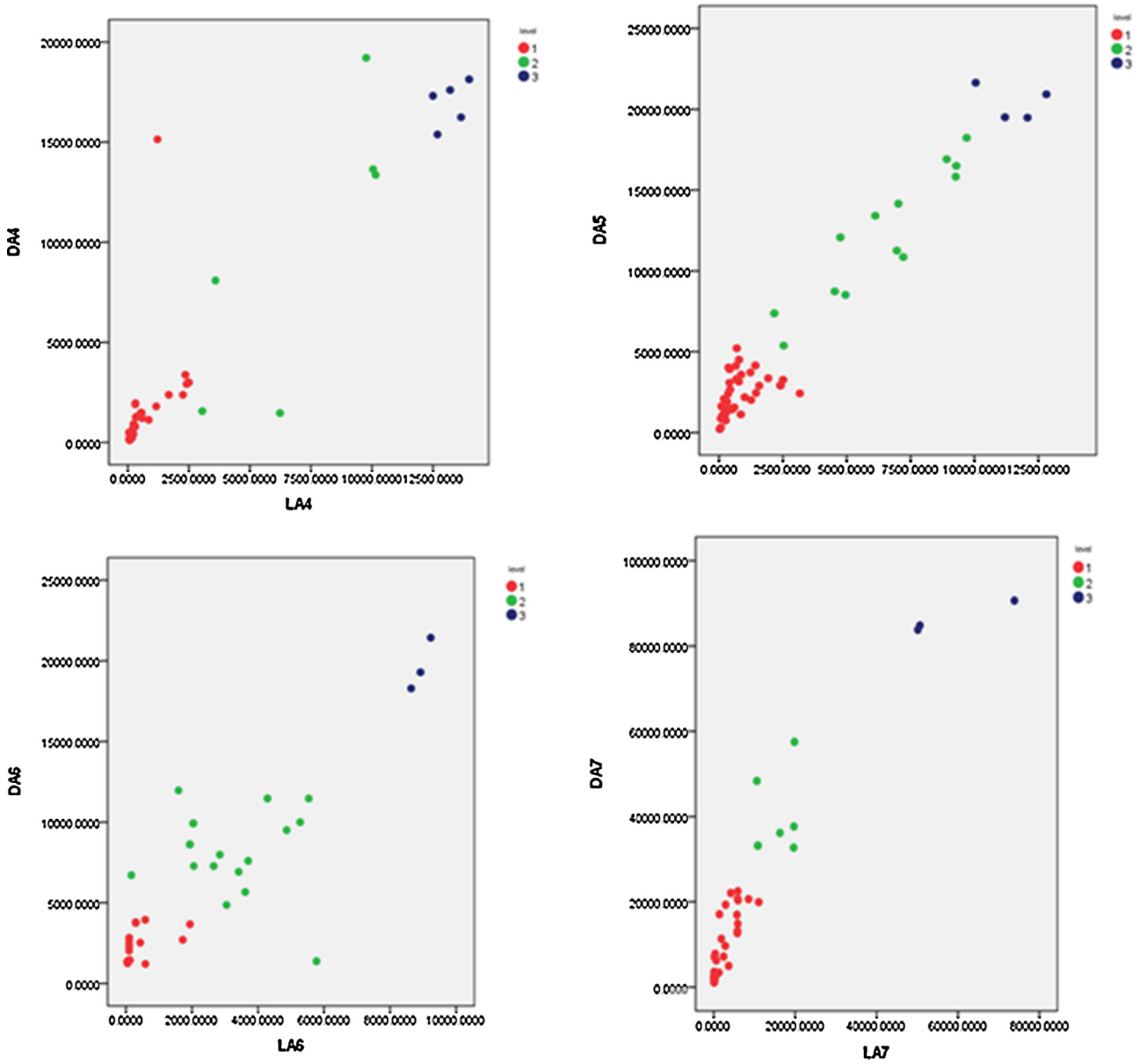

Fig. 4 – Cluster analysis of 4th, 5th, 6th and 7th decades with scatter plot showing clusters: red (population 1), green (population 2), and blue (population 3).

Table 3 – Mean numerical density of positive α-SMA cells (per μm^2) around the periacinar, periductular, perivascular, and peri-islar regions of the pancreas.

Decade	Periacinar[a]	Periductular[a]	Perivascular[a]	Peri-Islar[a]
Fourth	17.6 (4.60)	11.20 (2.3)	38.60 (2.5)	1.40 (0.74)
Fifth	48.4 (3.20)	22.20 (2.6)	58.0 (2.9)	4.0 (1.50)
Sixth	57.75 (7.12)	31.75 (4.19)	85.75 (9.12)	7.0 (1.80)
Seventh	125.25 (12.65)[*]	40.75 (6.50)[@]	94.00 (9.50)[$]	8.75 (1.65)[#]
Total	58.88 (9.22)	25.38 (3.13)	66.77 (6.03)	5.2 (0.93)

[*] $p = 0.002$ for 4th vs. 7th decades.
[@] $p = 0.004$ for 4th vs. 7th decades.
[$] $p = 0.002$ for 4th vs. 7th decades.
[#] $p = 0.012$ for 4th vs. 7th decades.
[a] Mean (SE).

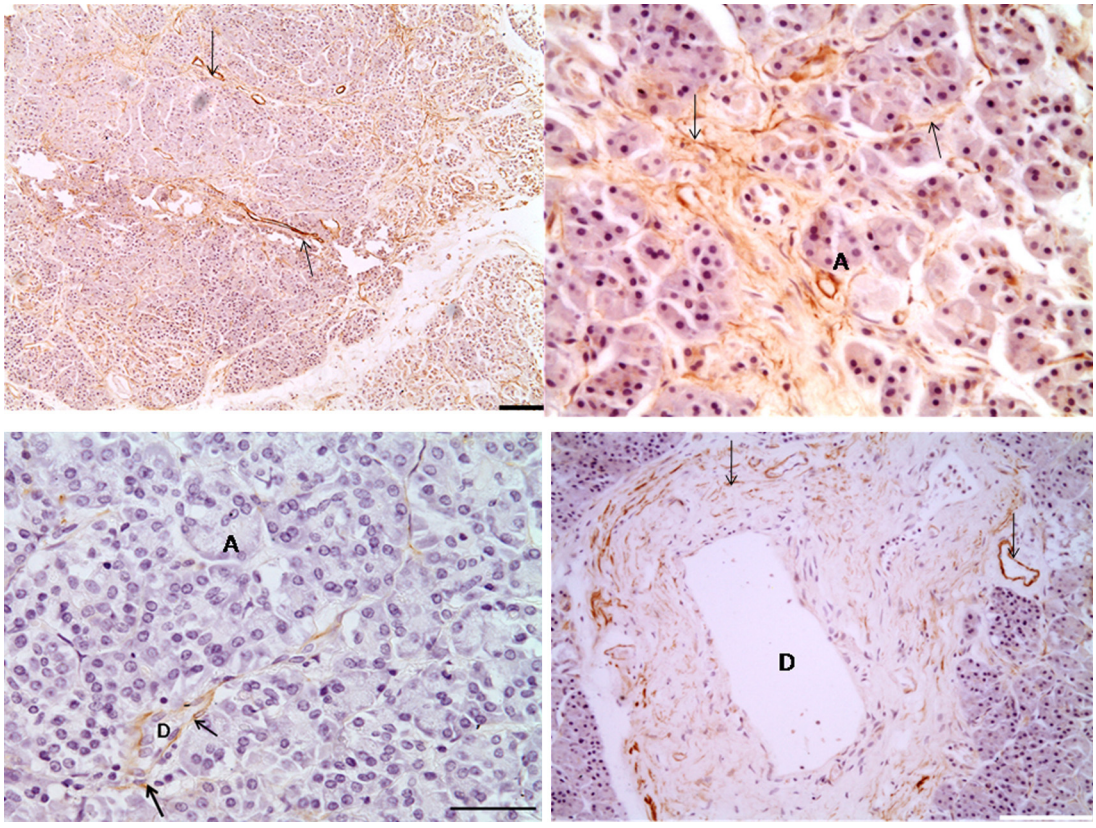

Fig. 5 – Photomicrographs of section of pancreas stained for α-SMA (brown cells) showing (a) low magnification (b) and high magnification (b) images of α-SMA positivity around the acini and blood vessels (c and d) around duct. Scale bar: (a) 200 μm, (b) 50 μm, (c) 20 μm, and (d) 50 μm.

Fibrosis in the human pancreas is associated with activated stellate cells[17] as α-SMA co-localized with mRNA, which conclusively proved that activated stellate cells were the principal source of collagen production in the fibrotic pancreas.[17] The results of the present study provide strong morphologic evidence in support of a similar involvement of α-SMA positive cells in pancreatic fibrogenesis. We also found that the density of α-SMA positive cells per unit area was significantly increased in their periacinar, periductular, and perivascular locations with increasing age. The density of α-SMA cells was maximum in the perivascular area, since the blood vessels have smooth muscle cells, which stained positive for α-SMA.[21] Positive α-SMA cells around the acini, seen in the present study, with increasing age suggesting that periacinar fibrosis is an age-related process. Hence, the increasing α-SMA positivity around the acini with associated fibrosis, with age indicates the predominant contribution of PSCs to fibrogenesis around the acini. Further, the density of α-SMA cells increased dramatically in the islets in the 7th decade. This may correlate with a higher incidence of glucose intolerance in the elderly. But this finding needs to be explored further.

In addition, we believe that this new classification of ducts based on unbiased morphometric data could become a useful tool in studies dealing with diseases that affect some subpopulations of ducts more than others.[18]

5. Conclusion

Morphometrically quantifiable changes occur in the architecture of the pancreas with aging. Whether these are primary or secondary to the fibrotic changes will be a subject of future studies. Even though pancreatic fibrosis in the elderly is clinically silent, it may be an important factor in gradual onset of endocrine and exocrine dysfunctions of the pancreas. Fibrosis with increasing age is due to dysregulation of ECM production that results from the activation of PSCs. Thus understanding the biology of the PSC may help to alter their function and control fibrotic changes in pancreas, in the future.

Conflicts of interest

The authors have none to declare.

Acknowledgements

The specimens were provided by the Department of Forensic Science AIIMS, for which we record our gratefulness.

REFERENCES

1. Gagliano N, Arosio B, Santambrogio D, et al. Age-dependent expression of fibrosis-related genes and collagen deposition in rat kidney cortex. *J Gerontol A Biol Sci Med Sci*. 2000;55: B365–B372.
2. Calabresi C, Arosio B, Galimberti L, et al. Natural aging, expression of fibrosis-related genes and collagen deposition in rat lung. *Exp Gerontol*. 2007;42:1003–1011.
3. Glaser J, Stienecker K. Pancreas aging: a study using ultrasonography. *Gerontology*. 2000;46:93–96.
4. Apte MV, Pirola RC, Wilson JS. Pancreatic stellate cells starring in normal and diseased pancreas. *Front Physiol*. 2012;3(344):1.
5. Apte MV, Park S, Phillips PA, et al. Desmoplastic reaction in pancreatic cancer: role of pancreatic stellate cells. *Pancreas*. 2004;29:179–187.
6. Kloppel G, Detlefsen S, Feyerabend B. Fibrosis of the pancreas: the initial tissue damage. Fibrosis of the pancreas: the initial tissue damage and the resulting pattern. *Virchows Arch*. 2004;445:1–8.
7. Kim JW, Ko SH, Cho JH, et al. Loss of beta cells with fibrotic islet destruction in type 2 diabetes mellitus. *Front Biosci*. 2008;13:6022–6033.
8. Pitchumoni CS, Glasser M, Saran RM, Panchacharam P, Thelmo W. Pancreatic fibrosis in chronic alcoholics and nonalcoholics without clinical pancreatitis. *Arm J Gastroenterol*. 1984;79(5):382–388.
9. Shimizu M, Hayashi T, Saitoh Y, Itoh H. Interstitial fibrosis in the pancreas. *Am J Clin Pathol*. 1989;91(5):531–534.
10. Anand BS, Vij JC, Mac HS, Chowdhury V, Kumar A. Effect of aging on the pancreatic ducts: a study based on endoscopic retrograde pancreatography. *Gastrointest Endosc*. 1989;35 (3):210–213.
11. Valderrama R, Navarro S, Campo E, et al. Quantitative measurement of fibrosis in pancreatic tissue. Evaluation of a colorimetric method. *Int J Pancreatol*. 1991;10(1):23–29.
12. Detlefsen B, Bernd S, Gunter F, Kloppel G. Pancreatic fibrosis associated with age and ductal papillary hyperplasia. *Virchows Arch*. 2005;447:800–805.
13. Bachem MG, Schneider E, Gross H. Identification, culture, and characterization of pancreatic stellate cells in rats and humans. *Gastroenterology*. 1998;115(2):421–492.
14. Omary MB, Lugea A, Lowe AW, Pandol SJ. The pancreatic stellate cell: a star on the rise in pancreatic diseases. *J Clin Invest*. 2007;117(1):50–59.
15. Lugea A, Nan L, French SW, Bezerra JA, Gukovskaya AS, Pandol SJ. Pancreas recovery following cerulein-induced pancreatitis is impaired in plasminogen-deficient mice. *Gastroenterology*. 2006;131:885–899.
16. Zimmermann A, Gloor B, Kappeler A, Uhl W, Friess H, Buchler MW. Pancreatic stellate cells contribute to regeneration early after acute necrotizing pancreatitis in humans. *Gut*. 2002;51:574–578.
17. Haber P, Keogh G, Apte M, et al. Activation of pancreatic stellate cells in human and experimental pancreatic fibrosis. *Am J Pathol*. 1999;155:1087–1095.
18. Fukumura Y, Suda K, Mitani K, Takase M, Kumasaka T. Expression of transforming growth factor beta by small duct epithelium in chronic, cancer-associated, obstructive pancreatitis: an in situ hybridization study and review of the literature. *Pancreas*. 2007;35(4):353–357.
19. Kreel L, Sandin B. Changes in pancreatic morphology associated with aging. *Gut*. 1973;14(12):962–970.
20. Schmitz-Moormann P, Thoma W, Hein J, Ihm P. Comparative radiological and morphological study of the human pancreas, morphometrical investigation of the human pancreatic duct system [Thoma W, Hein J, Ihm P, Author's Trans.]. *Anat Anz*. 1977;141(5):507–511.
21. Skalli O, Pelte MF, Peclet MC, Gabbiani G, Gugliotta P. Alpha smooth muscle actin a differential marker of smooth muscle cells, in microfilamentous bundles of pericytes. *J Histochem Cytochem*. 1989;37(3):315–321.
22. Allen-Mersh TG. Pancreatic ductal mucinous hyperplasia: distribution within the pancreas, and effect of variation in ampullary and pancreatic duct anatomy. *Gut*. 1988;26 (8):825–883.
23. Bhanot UK, Moller P. Mechanisms of parenchymal injury and signaling pathways in ectatic ducts of chronic pancreatitis: implications for pancreatic carcinogenesis. *Lab Investig*. 2009;89:489–497.
24. Hastier P, Buckley MJ, Dumas R, et al. A study of the effect of age on pancreatic duct morphology. *Gastrointest Endosc*. 1998;48(1):53–57.
25. Schmitz-Moormann P, Hein J. Changes of the pancreatic duct system associated with aging: their relations to parenchyma. *Virchows Arch A Pathol Anat Histol*. 1976;371 (2):145–152.
26. Stamm BH. Incidence and diagnostic significance of minor pathologic changes in adult pancreas at autopsy: a systematic study of 112 autopsies in patients without known pancreatic disease. *Human Pathol*. 1984;15(7): 677–683.